6-1994

Minimization of Temperature Effects of High-Birefringent Elliptical Fibers for Polarmetric Optical-Fiber Sensors

Feng Zhang
University of Waterloo

John W.Y. Lit
Wilfrid Laurier University, jlit@wlu.ca

Minimization of temperature effects of high-birefringent elliptical fibers for polarimetric optical-fiber sensors

Feng Zhang and John W. Y. Lit

The temperature dependence of polarization-maintaining fibers is a problem in polarimetric optical-fiber sensors. We report a novel method for making a temperature-insensitive, polarization-maintaining fiber, which may be used for the sensing part in a polarimetric strain sensor. The fiber has a double-clad elliptical core with built-in stresses in the core and cladding regions. To minimize the temperature sensitivity, the built-in stresses are balanced with the refractive-index differences and the core ellipticity properly chosen. The temperature and strain sensitivities of the fiber are calculated. A practical design and some potential applications of such a temperature-insensitive fiber with a high strain sensitivity are presented.

1. Introduction

Polarimetric fiber-optic sensors (PFOS's) have wider dynamic ranges; their system constructions are simpler than their interferometric counterparts.[1,2] Polarization-maintaining (PM) fibers play a key role in the PFOS as a sensing part and a leading head. Unfortunately the measurement of a slowly varying physical parameter by PFOS suffers from environmental fluctuations such as temperature, which limit the PFOS in practical uses.

A number of ways have been proposed to overcome the low-frequency environmentally induced instability of the DC quantity measurements of PFOS. Dakin and Wade[3] introduced a common mode rejection method by connecting two equal lengths of PM fibers with their polarization planes perpendicular to each other. Imai and Ohtsuka[4] used two identical PM fibers with a 90° optical axis difference parallel to each other to separate the temperature and bending effects. Kikuchi *et al.*[5] experimentally minimized the temperature sensitivity of built-in stress PM fiber by coating the fiber with additional layers. A theoretical analysis of such a fiber has been done by Mcdearmon[6] and Wang.[7]

In our previous paper[8] we analyzed and calculated the temperature and strain sensitivities of a high-birefringent, double-clad elliptical fiber without built-in stresses. We proposed a method to minimize those sensitivities by suitably selecting the fiber parameters: core ellipticity, refractive-index difference, and thickness of the inner cladding. In this paper we present a method for minimizing the temperature sensitivity of high-birefringent elliptical fibers with built-in stresses without increasing the fiber size; this is achieved by balancing the built-in stresses in the core and claddings of the fibers. In Section 2 we describe the structure, the birefringence, and the mode dispersion of the fiber. In Section 3 we derive the general formulas for the phase retardation between two eigenpolarizations caused by an arbitrary external perturbation to the fibers. We also discuss the effects of two special cases, temperature and axial strain, and derive the fiber sensitivities caused by these perturbations. In Section 4 we present a method for minimizing the temperature sensitivity of a PM fiber and give a design as an example of the temperature-insensitive fibers. We also present the strain sensitivity of fibers and show that it may be increased while the temperature sensitivity at a certain wavelength is reduced to zero. These fibers are suitable for fiber polarimetric strain sensors.

When this study was performed F. Zhang was with the Department of the Physics, (GWP)^2, University of Waterloo, Waterloo, Ontario N2L 3G1, Canada. He is now with Opto-Electronics, Inc., Oakville L6L 5K9, Canada. J. W. Y. Lit is with the Department of Physics and Computing, Wilfrid Laurier University, Waterloo, Ontario, N2L 3C5.

Received 8 April 1992.
0003-6935/94/163604-07$06.00/0.

2. Birefringence and Mode Dispersion of Elliptical Fibers

A. Structures and Parameters of Double-Clad Elliptical Fibers

A double-clad elliptical fiber that has an elliptical inner cladding and a circular outer cladding, as shown in Fig. 1(a), has the following parameters: a_1 and a_2 are the major axes of the core and the inner cladding; b_1 and b_2 are the minor axes of the core and the inner cladding; n_0, n_1, and n_2 are the refractive indices of the core, inner cladding, and outer cladding, respectively. In terms of elliptical coordinates ξ and η, the two boundaries of the inner cladding may be expressed by $\xi = \xi_1$ and $\xi = \xi_2$.

The refractive-index distribution in the fiber may be written as [see Fig. 1(b)]

$$n^2(\xi) = n_0^2[1 - 2\Delta_2 f(\xi)], \tag{1}$$

where

$$f(\xi) = \begin{cases} 0 & \xi < \xi_1 \\ \alpha h(\xi - \xi_1) & \xi_1 \le \xi < \xi_2, \\ h(\xi - \xi_2) & \xi \ge \xi_2 \end{cases} \tag{2}$$

$$h(x) = \begin{cases} 0 & x < 0 \\ 1 & z \ge 0, \end{cases} \qquad \alpha = \frac{\Delta_1}{\Delta_2} = \frac{n_0^2 - n_1^2}{n_0^2 - n_2^2}, \tag{3}$$

with

$$\Delta_1 = \frac{n_0^2 - n_1^2}{2n_0^2}, \qquad \Delta_2 = \frac{n_0^2 - n_2^2}{2n_0^2} \tag{4}$$

The ratios $R_x = a_2/a_1$ and $R_y = b_2/b_1$ may be introduced, and the normalized frequencies are defined as

$$V_x = ka_1 n_0 (2\Delta_2)^{1/2}, \qquad V_y = kb_1 n_0 (2\Delta_2)^{1/2}. \tag{5}$$

B. Birefringence and Mode Dispersion

Generally the birefringence of an elliptical fiber is partly due to geometry and partly due to built-in stresses. The geometry birefringence is contributed by the elliptical core. The normalized geometry birefringence is given by[9]

$$B^g = \frac{\delta\beta^g}{k} = \frac{2n_0\Delta_2^2}{V_y^4}\left[\frac{1}{W_y^4} - \frac{1}{(a_1/b_1)^4 W_x^4}\right]. \tag{6}$$

Here $W_x = w_x/a_1$ and $W_y = w_y/b_1$ are the normalized spot sizes and k is the wave number.

The geometric mode dispersion is[9]

$$\Delta\tau^g = \frac{1}{c}\frac{\mathrm{d}(\delta\beta^g)}{\mathrm{d}k} = \frac{2n_0\Delta_2^2}{c}\frac{\mathrm{d}}{\mathrm{d}V_y}\left\{\frac{1}{V_y^3}\left[\frac{1}{W_y^4} - \frac{1}{(a_1/b_1)^4 W_x^4}\right]\right\}. \tag{7}$$

The normalized birefringence B^s resulting from built-in stress in a double-clad elliptical fiber is caused by geometry asymmetry and by the different thermal expansions of the core, inner cladding, and outer cladding (α_0, α_1, and α_2). It is made up of two parts: B_0^s caused by stress differences in the core and B_1^s caused by stress differences in the inner cladding[10,11]:

$$B^s = B_0^s + B_1^s \tag{8}$$

with

$$B_0^s = b(V_y)\frac{EC}{1-\nu}\Delta\alpha_1\Delta T_1\frac{a_1 - b_1}{a_1 + b_1}, \tag{9}$$

and

$$B_1^s = \frac{EC}{1-\nu}\Delta\alpha_2\Delta T_2\frac{a_2 - b_2}{a_2 + b_2}, \tag{10}$$

$$C = \frac{n_0^3}{2E}(p_{11} - p_{12})(1 + \nu), \tag{11}$$

$$\Delta\alpha_1 = \alpha_0 - \alpha_1, \qquad \Delta\alpha_2 = \alpha_1 - \alpha_2, \tag{12}$$

$$\Delta T_1 = T_r - T_{s0}, \qquad \Delta T_2 = T_r - T_{s1}, \tag{13}$$

where E is the Young's modulus, ν is the Poisson ratio of fused silica, p_{11} and p_{12} are the strain-optic coefficients, $b(V_y)$ is the normalized propagation constant, T_r is the room temperature, and T_{s0} and T_{s1} are the softening temperatures of the core and inner cladding.

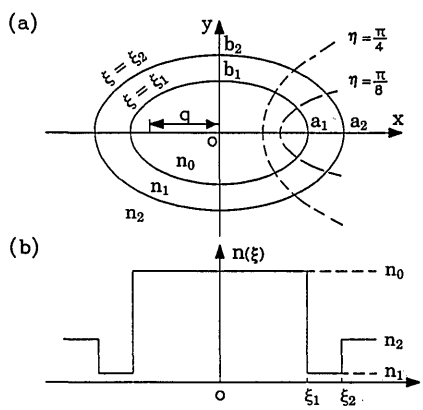

Fig. 1. (a) Schematic diagram of a double-clad elliptical fiber with an elliptical inner cladding and a circular outer cladding. (b) Refractive-index distribution in the radial direction.

3. Phase Retardation

A. General Formulas

The phase retardation between two eigenmodes HE_{11}^x and HE_{11}^y in a fiber length L is

$$\delta\phi = \delta\beta L, \tag{14}$$

where

$$\delta\beta = \delta\beta^g + \delta\beta^s, \qquad \delta\beta^s = \delta\beta_0{}^s + \delta\beta_1{}^s, \tag{15}$$

and the stress birefringences are $\delta\beta_0{}^s = kB_0{}^s$, $\delta\beta_1{}^s = kB_1{}^s$, and $\delta\beta^s = kB^s$.

If the fiber is perturbed by a physical quantity ζ_p, Eq. (14) gives

$$\frac{d(\delta\phi)}{d\zeta_p} = \frac{d(\delta\beta)}{d\zeta_p} L + \frac{dL}{d\zeta_p}\delta\beta. \tag{16}$$

1. *Phase Retardation Resulting from Geometry Birefringence*

First, we consider only the geometry contribution to the birefringence of an elliptical fiber. $\delta\beta^g$ is a function of normalized frequency V_y and ellipticity e of the elliptical fiber core:

$$\frac{d(\delta\beta^g)}{d\zeta_p} = \frac{\partial(\delta\beta^g)}{\partial V_y}\frac{dV_y}{d\zeta_p} + \frac{\partial(\delta\beta^g)}{\partial e}\frac{de}{d\zeta_p}. \tag{17}$$

The general formula for the phase shift caused by any physical perturbation is given by[8]

$$\begin{aligned}\frac{d(\delta\phi^g)}{d\zeta_p} = \frac{k}{V_y}\frac{\partial V_y}{\partial\zeta_p}\frac{\partial(\delta\beta^g)}{\partial k} L + \frac{\partial(\delta\beta^g)}{\partial e}\frac{de}{d\zeta_p} L + \left\{\frac{1}{n_0 - n_2}\right.\\ \times \frac{\partial(n_0 - n_2)}{\partial\zeta_p} - \left[1 - \frac{\lambda}{n_0 - n_2}\frac{\partial(n_0 - n_2)}{\partial\lambda}\right]\\ \left.\times \frac{1}{V_y}\frac{\partial V_y}{\partial\zeta_p} + \frac{1}{L}\frac{dL}{d\zeta_p}\right\}\delta\beta^g L.\end{aligned} \tag{18}$$

Here we can see that the phase retardation depends not only on the change of the fiber parameters caused by perturbation but also on the waveguide dispersion given in Eq. (7) and the material dispersions that may be obtained from the Sellmeier equation:

$$\frac{dn_i}{d\lambda} = -\frac{\lambda}{n_i}\sum_{s=1}^{3}\frac{A_s\lambda_s{}^2}{(\lambda^2 - \lambda_s{}^2)^2}, \tag{19}$$

where the parameters A_s and λ_s are given by an rms fit to experimental data.[13]

2. *Phase Retardation Caused by Built-in Stress Birefringence*

The birefringence caused by built-in stress is a function of normalized frequency V_y and stress differences between fast and slow optical axes $\delta\sigma$, i.e.,

$$\frac{d(\delta\beta^s)}{d\zeta_p} = \frac{\partial(\delta\beta^s)}{\partial V_y}\frac{dV_y}{d\zeta_p} + \frac{\partial(\delta\beta^s)}{\partial(\delta\sigma)}\frac{d(\delta\sigma)}{d\zeta_p}, \tag{20}$$

$$\frac{d(\delta\phi^s)}{d\zeta_p} = \frac{\partial(\delta\beta^s)}{\partial V_y}\frac{dV_y}{d\zeta_p} L + \frac{\partial(\delta\beta^s)}{\partial(\delta\sigma)}\frac{d(\delta\sigma)}{d\zeta_p} L + \frac{dL}{d\zeta_p}\delta\beta^s. \tag{21}$$

We now discuss two important effects, the temperature and axial strain effects.

B. Temperature Effects

1. *Response of Geometry Birefringence*

First, here we neglect the built-in stresses of the fiber. Temperature variations may change the dimensions and refractive indices of a fiber. Assuming the fiber to have homogeneous thermal materials and setting $\zeta_p = T$, we can obtain the temperature sensitivity[8]

$$\frac{d(\delta\phi^g)}{LdT} = k(\alpha_n + \alpha_e)\left[\frac{\partial(\delta\beta^g)}{\partial k} + \frac{\lambda}{n_0 - n_2}\frac{\partial(n_0 - n_2)}{\partial\lambda}B^g\right], \tag{22}$$

where α_n and α_e are, respectively, the average temperature coefficient of the refractive index and the average coefficient of thermal expansion. Thus the phase retardation between two eigenmodes caused by temperature depends on the waveguide dispersion $\partial(\delta\beta^g)/\partial k$ and the material dispersion $\partial(n_0 - n_2)/\partial\lambda$. Because the second term in Eq. (22) is much smaller than the first,[8] it is ignored. Hence Eq. (22)is simplified to

$$\frac{d\delta\phi^g}{LdT} \approx k(\alpha_n + \alpha_e)\frac{\partial(\delta\beta^g)}{\partial k}, \tag{23}$$

2. *Response of Built-in Stress Birefringence*

Substituting $\zeta_p = T$ into Eq. (20), we have

$$\frac{d(\delta\beta^s)}{dT} = \frac{\partial(\delta\beta^s)}{\partial V_y}\frac{dV_y}{dT} + \frac{\partial(\delta\beta^s)}{\partial(\delta\sigma)}\frac{d(\delta\sigma)}{dT}, \tag{24}$$

Then substitution of $\delta\beta^s = kB^s$ gives

$$\frac{1}{k}\frac{d(\delta\beta^s)}{dT} = \left(\frac{B^s}{V_y} + \frac{\partial B^s}{\partial V_y}\right)\frac{dV_y}{dT} + \frac{\partial B^s}{\partial(\delta\sigma)}\frac{d(\delta\sigma)}{dT}. \tag{25}$$

Using Eqs. (8)–(10) and $(1/V_y)(dV_y/dT) = \alpha_n + \alpha_e$,[8] we obtain the temperature sensitivity of the built-in stress birefringence:

$$\begin{aligned}\frac{1}{k}\frac{d(\delta\beta^s)}{dT} = V_y(\alpha_n + \alpha_e)\left[\frac{B^s}{V_y} + \frac{b'(V_y)}{b(V_y)}B_0{}^s\right]\\ + \left(\frac{B_0{}^s}{\Delta T_1} + \frac{B_1{}^s}{\Delta T_2}\right).\end{aligned} \tag{26}$$

The phase retardation is

$$\begin{aligned}\frac{1}{L}\frac{d(\delta\phi^s)}{dT} = k(2\alpha_n + \alpha_e)\left[B^s + \frac{b'(V_y)}{b(V_y)}V_y B_0{}^s\right]\\ + k\left(\frac{B_0{}^s}{\Delta T_1} + \frac{B_1{}^s}{\Delta T_2}\right).\end{aligned} \tag{27}$$

For fused silica, because $\alpha_e = 0.5 \times 10^{-6}$ and $\alpha_n = 10^{-5}$ and $1/\Delta T_1, 1/\Delta T_2 \sim -10^{-3}/°C$, the first term in Eq. (27) is ~2 orders smaller than the second term.

The equation can be simplified to

$$\frac{1}{L}\frac{d(\delta\phi^s)}{dT} \approx k\left(\frac{B_0^s}{\Delta T_1} + \frac{B_1^s}{\Delta T_2}\right). \quad (28)$$

The phase retardation caused by built-in stresses is proportional to the sum of the birefringences B_0^s and B_1^s divided by their respective ΔT's.

C. Axial Strain Effects

1. *Response of Geometry Birefringence*

We assume that the fiber has a homogeneous elasticity if there were no built-in stresses in the fiber and that the expansion dL is much smaller than L. Setting $d\zeta_p = dL$, we can obtain the axial strain sensitivity as[8]

$$\frac{d(\delta\phi^g)}{dL} = -k(\nu + C_{st})\left[\frac{\partial(\delta\beta^g)}{dk} + \frac{\lambda}{(n_0 - n_2)}\frac{\partial(n_0 - n_2)}{\partial\lambda}B^g\right] + k(1 + \nu - C_{st})B^g, \quad (29)$$

where

$$C_{st} = n_0^2[p_{12} - \nu(p_{11} + p_{12})]. \quad (30)$$

2. *Response of Built-in Stress Birefringence*

With $d\zeta_p = dL$, Eq. (20) becomes

$$\frac{d(\delta\beta^s)}{dL} = \frac{\partial(\delta\beta^s)}{\partial V_y}\frac{dV_y}{dL} + \frac{\partial(\delta\beta^s)}{\partial(\delta\sigma)}\frac{d(\delta\sigma)}{dL}. \quad (31)$$

Then, when $\delta\beta^s = kB^s$ is used,

$$\frac{1}{k}\frac{d(\delta\beta^s)}{dL} = \left(\frac{B^s}{V_y} + \frac{\partial B^s}{\partial V_y}\right)\frac{dV_y}{dL} + \frac{\partial B^s}{\partial(\delta\sigma)}\frac{d(\delta\sigma)}{dL}. \quad (32)$$

With the help of Eqs. (8)–(10), (30), and (33),[7]

$$\frac{1}{V_y}\frac{dV_y}{dL} \approx -\frac{\nu}{L} - \frac{{n_1}^2}{L}[p_{12} - \nu(p_{11} - p_{12})]; \quad (33)$$

the first term on the right of Eq. (32) is given by

$$\left(\frac{B^s}{V_y} + \frac{\partial B^s}{\partial V_y}\right)\frac{dV_y}{dL} = -\frac{(\nu + C_{st})}{L}\left[B^s + \frac{b'(V_y)}{b(V_y)}V_y B_0^s\right]. \quad (34)$$

The second term needs more discussion. Stretching a fiber in the z direction with a uniform strain ε_z will result in free strains in the transverse x and y directions, $\varepsilon_x = \varepsilon_y = -\nu\varepsilon_z$, which are analogous to the free thermal strains $\varepsilon_x = \varepsilon_y = \Delta\alpha\Delta T$ occurring as the fiber cools. Because $B_0^s \propto \Delta\alpha_1\Delta T_1$ and $B_1^s \propto \Delta\alpha_2\Delta T_2$, the change of birefringence after stretching may be approximately given by[14]

$$\Delta B_0^s = -\frac{\Delta\nu_1\varepsilon_z}{\Delta\alpha_1\Delta T_1}B_0^s, \quad (35)$$

$$\Delta B_1^s = -\frac{\Delta\nu_2\varepsilon_z}{\Delta\alpha_2\Delta T_2}B_1^s \quad (36)$$

or

$$\frac{\Delta B_0^s}{\Delta L} = -\frac{\Delta\nu_1}{\Delta\alpha_1\Delta T_1 L}B_0^s, \quad (37)$$

$$\frac{\Delta B_1^s}{\Delta L} = -\frac{\Delta\nu_2}{\Delta\alpha_2\Delta T_2 L}B_1^s, \quad (38)$$

with $\Delta\nu_1 = \nu_0 - \nu_1$ and $\Delta\nu_2 = \nu_1 - \nu_2$, where ν_0, ν_1, and ν_2 are the Poisson ratios of the core, inner cladding, and outer cladding, respectively. By substituting Eqs. (34)–(38) into Eq. (32), we have

$$\frac{d(\delta\beta^s)}{dL} = -\frac{k(\nu + C_{st})}{L}\left[B^s + \frac{b'(V_y)}{b(V_y)}V_y B_0^s\right] - \frac{k}{L}\left(\frac{\Delta\nu_1}{\Delta\alpha_1\Delta T_1}B_0^s + \frac{\Delta\nu_2}{\Delta\alpha_2\Delta T_2}B_1^s\right), \quad (39)$$

and the sensitivity of strain is

$$\frac{d(\delta\phi^s)}{dL} = k\left\{(1 - \nu - C_{st})B^s - \left[\frac{\Delta\nu_1}{\Delta\alpha_1\Delta T_1} + (\nu + C_{st})\frac{b'(V_y)}{b(V_y)}V_y\right]B_0^s - \frac{\Delta\nu_2}{\Delta\alpha_2\Delta T_2}B_1^s\right\}. \quad (40)$$

4. Design of Temperature-Insensitive Fibers

A. Temperature Insensitivity

Equations (23) and (28) give the temperature sensitivities of the phase retardation between two eigenpolarizations of an elliptical fiber caused, respectively, by the effects of fiber geometry and built-in stresses. The total phase retardation caused by temperature can be obtained by adding the two effects:

$$\frac{d(\delta\phi)}{LdT} = \frac{d(\delta\phi^g)}{LdT} + \frac{d(\delta\phi^s)}{LdT}. \quad (41)$$

If the birefringence of an elliptical fiber is caused solely by the fiber geometry, the temperature sensitivity can be minimized by suitably selecting the fiber parameters: core ellipticity, refractive-index difference, and/or thickness of the inner cladding.[8]

In the more general case the birefringence of an elliptical fiber is composed of a geometrical component B^g, a core-stress component B_0^s, and a cladding-stress component B_1^s. All these birefringences contribute to the temperature sensitivity of the fiber. From Eqs. (23) and (28) we see that the temperature sensitivity depends on the waveguide dispersion $\partial(\delta\beta^g)/\partial k$ and the stress birefringences B_0^s and B_1^s. Here $\partial(\delta\beta^g)/\partial k$ and B_0^s are frequency dependent. If we can move the zero points of $\partial(\delta\beta^g)/\partial k$ and $B_0^s/\Delta T_1 + B_1^s/\Delta T_2$ to the same V_y, we can make the fiber insensitive to temperature at a certain wavelength. The zero points of $\partial(\delta\beta^g)/\partial k$ can be controlled by selecting the fiber parameters: core ellip-

ticity, refractive-index difference, and thickness of the inner cladding. If we introduce an inner elliptical cladding with a thermal expansion coefficient that is different from those of the core and outer cladding, the built-in stresses in the core and cladding will produce birefringences B_0^s and B_1^s. The signs of B_0^s and B_1^s can be the same or different depending on the thermal expansion coefficients of the core and inner and outer claddings of the fiber. Fiber cores are generally made by doping GeO_2 in fused silica SiO_2, which is the outer cladding material, resulting in $\alpha_0 > \alpha_1$. For the inner cladding one can increase the thermal expansion coefficient by dopants such as P_2O_5 and B_2O_3.[15] These are common materials used to produce the stress-induced components in PM fibers. If we control the doping and make $\alpha_0 > \alpha_1 > \alpha_2$, both the core and cladding will have compressive stresses, and B_0^s and B_1^s will add together [see Eqs. (9) and (10)]. Another group of dopants, such as TiO_2 and F_2, can decrease the thermal expansion coefficient.[11,15] If $\alpha_0 > \alpha_1 < \alpha_2$, there is compressive stress in the core but an expansive stress in the cladding, resulting in B_0^s and B_1^s having opposite signs. Hence $B_0^s/\Delta T_1 + B_1^s/\Delta T_2$ can be made zero at a certain V_y by controlling the doping and ellipticity of the inner cladding.

In the following we give an example of the design of a temperature-insensitive fiber. We dope the fiber core with GeO_2, which increases the refractive index and the thermal expansion coefficient. For the inner cladding we use TiO_2 doping to decrease the thermal expansion coefficient. The doping quantities, refractive indices, and thermal expansion coefficients are given in Table 1.[15] From the table and Eq. (4) the relative refractive-index differences are $\Delta_1 = 0.01$ and $\Delta_2 = 0.02$. By choosing $a_1/b_1 = 2.0$ and $R_x > 1.4$ (the geometry birefringence resulting from the cladding can be ignored[9]), we shall have the zero dispersion point at $V_y = 1.767$. Hence we have to make the temperature sensitivity caused by built-in stress at $V_y = 1.767$ zero, so that the total phase retardation caused by temperature will be zero. From Table 1 the difference between the thermal expansion coefficients of the core and inner cladding and that between the inner cladding and outer cladding are, respectively,

$$\Delta\alpha_1 = \alpha_{GeO_2} - \alpha_{TiO_2} = 1.7 \times 10^{-6},$$

$$\Delta\alpha_2 = \alpha_{TiO_2} - \alpha_{SiO_2} = -0.3 \times 10^{-6}.$$

If ΔT_1, $\Delta T_2 \sim 1000°C$, $\Delta\nu_1$, $\Delta\nu_2 \sim 0.02$, and $a_2/b_2 = 4.38$, we have $B_0^s = -B_1^s = 0.72 \times 10^{-4}$ at $V_y = 1.767$.

Table 1. Doping Quantities, Refractive Indices, and Thermal Expansion Coefficients for the Temperature-Insensitive Fiber Designed

Dopant	Mol. %	n	α ($\times 10^{-6}$)
GeO_2	22	1.490	1.9
TiO_2	3.5	1.475	0.2
SiO_2	—	1.459	0.5

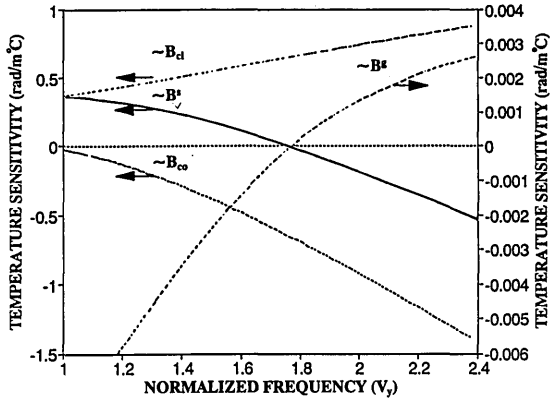

Fig. 2. Temperature sensitivities resulting from B^g, B_{c0}^s, B_{c1}^s, and the total stress birefringence B^s as functions of normalized frequency V_y, $n_0 = 1.49$, $\Delta_1 = 0.01$, $\Delta_2 = 0.02$, $a_1/b_1 = 2.0$, $a_2/b_2 = 4.38$, and $b_1 = 0.845$ μm, $\lambda = 0.633$ μm.

Therefore, when $V_y = 1.767$ (within the single-mode range), the temperature sensitivity of the fiber is zero. Figure 2 shows the temperature sensitivities resulting from B^g [given by Eq. (22)], B_0^s [given by the first term in Eq. (28)], B_1^s [the second term in Eq. (28)], and the total stress birefringence B^s [given by Eq. (28)] as functions of the normalized frequency V_y. The temperature sensitivity of B^g is ~2 orders of magnitude smaller than those of stress-induced birefringences, but it may be the main effect when the resultant temperature sensitivity resulting from all stresses is zero. Our design above reduces both types of temperature sensitivity to zero, resulting in a fiber that is independent of temperature fluctuations.

B. Axial Strain Sensitivity

The axial strain sensitivities of an elliptical fiber caused by geometry and by built-in stress are given by Eqs. (29) and (40), respectively. The total phase retardation resulting from strain can be obtained by adding Eqs. (29) and (40). Figure 3 shows the axial strain sensitivities caused by B^g [given by Eq. (29)], B_0^s [given by the B_0^s term in Eq. (40)], B_1^s [given by the B_1^s term in Eq. (40)], and B^s [given by Eq. (40)] as functions of V_y for the fiber described in Subsection 4.

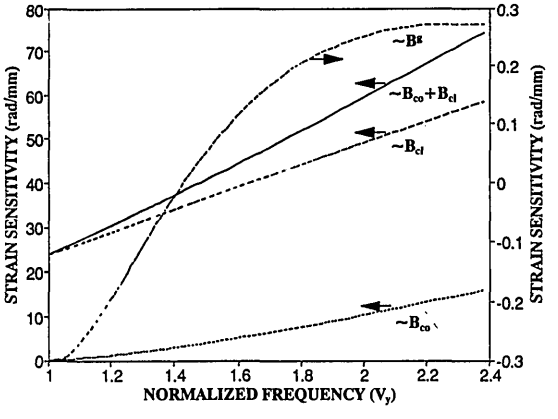

Fig. 3. Strain sensitivities resulting from B^g, B_{c0}^s, B_{c1}^s, and B^s as functions of normalized frequency V_y. Fiber parameters are the same as those in Fig. 2.

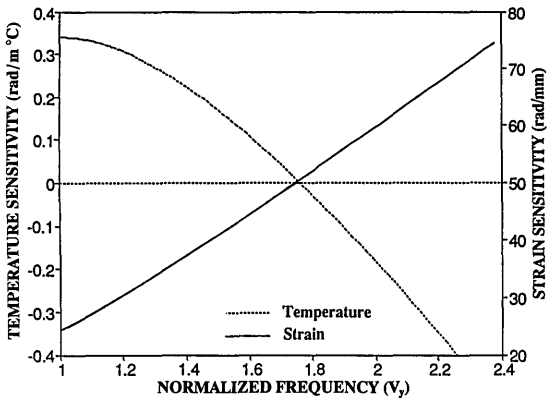

Fig. 4. Temperature and strain sensitivities as functions of normalized frequency V_y. The fiber parameters are the same as those in Fig. 2.

Built-in stresses enhance the axial-strain sensitivity by ~2 orders of magnitude. In our design the strain sensitivities caused by built-in stresses reinforce one another.

If the fiber is used in a polarimetric strain sensor, it must be designed with the highest strain sensitivity and the smallest temperature sensitivity. This may be realized by optimizing the fiber parameters. Figure 4 shows the total sensitivities of temperature and strain of the fiber as functions of the normalized frequency V_y. The strain sensitivity is ~50 rad/mm with a zero temperature sensitivity at $V_y = 1.767$, which is within the single-mode region.

5. Potential Applications of Temperature-Insensitive PM Fibers in Sensors

Strain measurement is of special importance because many primary measurands (e.g., bending, pressure, vibration, flow rate, electric and magnetic fields, acceleration) may be converted to displacements and hence to fiber strain. However, the measurement of quasi-static strain seriously suffers from environmental fluctuations, especially temperature. The temperature-insensitive PM fibers with a large strain sensitivity can be applied to the measurement of slowly varying (<0.05-Hz) strain with the help of polarimetry.

A. Smart Structures and Skins

Embedded fiber-optic sensors can monitor the mechanical characteristics of composite structures to produce smart structures.[16,17] Composite materials are now being used increasingly in a wide range of situations such as ships and submersibles, buildings and bridges, and aerospace vehicles and structures. Temperature-insensitive PM fibers with a large strain sensitivity are good candidates to be embedded in composite structures for the measurement of strain or vibration in the structures. When the fiber is embedded in the materials, an additional strain will act on the fiber. The fiber design has to consider the fiber and the structure properties.

B. Fiber-Optic Sensor Coatings

Coating materials applied as jackets to a single-mode optical fiber in an interferometric sensor usually play an important role in determining the fiber sensitivity and dynamic response to a particular field or parameter.[18] Similarly, the widespread application of polarimetric fiber-optic sensor technology depends significantly on the phase shift caused by a particular environmental parameter being effectively controlled and optimized by the use of suitable coatings for PM fibers.

The temperature-insensitive PM fibers coated with piezoelectric materials (PVF_2, copolymers), magnetostrictive materials (nickel alloys, metallic glass), elastomers (polystyrene, nylon), and so on have the potential to measure electric fields, magnetic fields, acoustic fields, etc. The coating materials can transduce and magnify the particular measurand fields to displacement and then to strain in the fiber. Using temperature-insensitive PM fibers and polarimetry, one can measure the fields that may have very low frequency changes.

C. Fiber-Optic Sensors Using Transducers

A number of physical quantities, such as electric and magnetic fields, current, pressure, vibration, flow rate, acceleration, can be changed to fiber strain by means of electric, magnetic, and mechanical transducers.[18] For example, a magnetostrictive tube, mandrel, or strip may convert magnetic fields to the strain of fibers bonded onto them. Suitably designed mechanical devices may transduce pressure, vibration, flow, and acceleration to fiber strains. These applications depend on the design of the particular transducers.

6. Conclusion

A double-clad elliptical fiber with built-in stresses can be designed as a temperature-insensitive PM fiber. This is achieved by suitably selecting doping materials for the core, inner cladding, and outer cladding to produce different thermal expansion coefficients. We have discussed in detail the design of the temperature-insensitive fibers with high strain sensitivities, suitable for polarimetric strain sensors. An example of the fiber design is given; a strain sensitivity of 50 rad/mm is obtained with a zero-temperature sensitivity. Finally, the potential applications of the temperature-insensitive fibers in polarimetric strain sensors, smart structures, and skins are discussed.

John W. Y. Lit is also affiliated with the Department of Physics, $(GWP)^2$, **Author queried** and the Department of Electric Engineering, University of Waterloo. This research is supported by the Ontario Laser and Lightwave Research Centre and by the Natural Sciences and Engineering Research Council of Canada.

References

1. A. D. Kersey, M. A. Davis, and M. J. Marrone, "Differential polarimetic fiber-optic sensor configuration with dual wavelength operation," Appl. Opt. **28**, 204–206 (1989).

2. S. C. Rashleigh, "Fiber-optic sensors with reduced sensitivity to environmental perturbations," Appl. Opt. **20,** 1498–1499 (1981).
3. J. P. Dakin and C. A. Wade, "Compensated polarimetric sensor using polarization-maintaining fiber in a differential configuration," Electron. Lett. **20,** 51–53 (1984).
4. Y. Imai and Y. Ohtsuka, "Compensated sensing based on retardation characteristics in a bent birefringent fiber," Appl. Opt. **25,** 4444–4447 (1986).
5. Y. Kikuchi, R. Yamauchi, M. Akiyama, O. Fukuda, and K. Inada, "Polarimetric strain and pressure sensors using temperature-independent polarization maintaining optical fiber," in *Second International Conference on Optical Fiber Sensors,* R. T. Kersten and R. Kist, eds., Proc. Soc. Photo-Opt. Instrum. Eng. **514,** 395–398 (1984).
6. G. F. Mcdearmon, "Theoretical analysis of the minimization of the temperature sensitivity of a coated optical fiber in a fiber-optic polarimeter," J. Lightwave Technol. **LT-8,** 51–55 (1990).
7. D. Wang, "Thermal stability of intrinsic stress birefringence in optical fibers," J. Lightwave Technol. **LT-8,** 1757–1761 (1990).
8. F. Zhang and J. W. Y. Lit, "Temperature and strain sensitivities of high-birefringent elliptical fibers," Appl. Opt. **31,** 1239–1243 (1992).
9. F. Zhang and J. W. Y. Lit, "Polarization characteristics of double-clad elliptical fibers," Appl. Opt. **29,** 5336–5342 (1990).
10. W. Eickhoff, "Stress-induced single-polarization single-mode fiber," Opt. Lett. **7,** 629–631 (1982).
11. S. C. Rashleigh, "Origins and control of polarization effects in single-mode fibers," J. Lightwave Technol. **LT-1,** 312–331 (1983).
12. D. Gloge, "Weakly guiding fibers," Appl. Opt. **10,** 2252–2258 (1971).
13. L. E. Sutton and O. N. Stavroudis, "Fitting refractive index data by least squares," J. Opt. Soc. Am. **51,** 901–905 (1961).
14. M. P. Varnham, A. J. Barlow, D. N. Payne, and K. Okamoto, "Polarimetric strain gauges using high birefringence fiber," Electron. Lett. **19,** 669–670 (1983).
15. S. E. Miller and A. G. Chynoweth, *Optical Fiber Telecommunications* (Academic, New York, 1979).
16. R. M. Measures, "Fiber optic sensors—the key to smart structures," in *Fibre Optics '89,* P. McGeehin, ed., Proc. Soc. Photo-Opt. Instrum. Eng. **1120,** 161–174 (1989).
17. E. Udd, ed., *Fiber Optic Smart Structures and Skins II,* Proc. Soc. Photo-Opt. Instrum. Eng. **1170** (1989).
18. R. P. D. Paula, "Fiber optic sensor overview," in *Fiber Optic and Laser Sensors III,* E. L. Moore and O. G. Ramer, eds., Proc. Soc. Photo-Opt. Instrum. Eng. **566,** 2–15 (1985).